Bioelectrochemistry 150 (2023) 108365

Contents lists available at ScienceDirect

Bioelectrochemistry

journal homepage: www.journals.elsevier.com/bioelectrochemistry

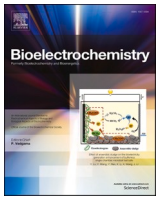

Electrochemiluminescence (ECL) biosensor based on tris(2,2′-bipyridyl) ruthenium(II) with glucose and lactate dehydrogenases encapsulated within alginate hydrogels

Lucia Simona Ferraraccio [a], Paolo Bertoncello [a,b,*]

[a] Department of Chemical Engineering, Faculty of Science and Engineering, Swansea University, Bay Campus, Crymlyn Burrows, Swansea SA1 8EN, United Kingdom
[b] Centre for NanoHealth, Swansea University, Singleton Campus, Swansea SA2 8PP, United Kingdom

ARTICLE INFO

Keywords:
Enzymes
Electrochemiluminescence
Bioelectrochemistry
Biosensors
Glucose dehydrogenase
Lactate dehydrogenase

ABSTRACT

Two dehydrogenase enzymes (glucose, GDH, and lactate, LDH, dehydrogenases) encapsulated within alginate hydrogels were deposited on glassy carbon electrodes. The as-prepared enzyme modified alginate hydrogels were utilized as electrochemiluminescence (ECL)-based biosensors for the indirect detection of glucose and lactic acid upon reaction between NADH and tris(2,2′-bipyridyl) ruthenium (II) $[Ru(bpy)_3]^{2+}$. The ECL response was obtained from the redox reaction between the substrate, the cofactor NAD^+ and the encapsulated enzyme. The production of NADH resulting from the enzymatic reaction led to the ECL emission upon reaction with $[Ru(bpy)_3]^{2+}$. The biosensors showed good stability and repeatability, with linear range between 0.56 and 4.2 μM and limit of detection of 0.84 μM for glucose, and linear range between 5 and 30 μM with a limit of detection of 2.52 μM for lactic acid. These ECL-based biosensors showed good sensitivity when tested in the presence of common interfering species. These biosensors were utilized in artificial sweat and were characterized by good reproducibility and repeatability. The results herein presented suggest that the dehydrogenases encapsulated within alginate hydrogels have potential for the development of biocompatible sensors for detection of glucose and lactic acid in physiological fluids.

1. Introduction

Nowadays, the demand for real-time, non-invasive, and low-cost biosensors continues to drive the bioanalytical research towards the development of highly sensitive and selective devices [1–3]. Of particular interest is the clinical diagnostic area, where the need of novel sensors based on the enzymatic detection represents a new method for reliable and precise detection of vital parameters such as glucose [4], lactic acid [5,6], and cholesterol [7]. Electrochemiluminescence (ECL) represents one of the most used tools for the chemical analysis and detection of these parameters due to excellent properties such as high sensitivity, optimal spatial and temporal control, reproducibility, and simplicity of the apparatus [8–10]. In particular, $[Ru(bpy)_3]^{2+}$ represents the most used luminophore due to its capability to produce ECL with several molecules such as amines (especially tripropylamine, TPrA) [11,12], amino acids [13], NADH [14], and oxalate [15]. The ECL of $[Ru(bpy)_3]^{2+}$ has been widely used for monitoring the enzymatic activity of dehydrogenase using NADH as coreactant [2]. Hence, the ECL emission represents a tool for monitoring the concentration of the substrates which are directly related to the variation of the NADH concentration due to the dehydrogenase activity. For this reason, the ECL mechanism involving $[Ru(bpy)_3]^{2+}$ and NADH has been employed in bioanalytical chemistry for ECL detection of alcohol [16,17].

Different methods for the immobilization of the enzymes are reported in literature in order to improve the catalytic efficiency and selectivity and to protect the enzymes from environmental changes like pH, temperature and solvents added to the electrolytic solution[18]. For example, the detection of ethanol and NADH has been achieved by immobilizing the alcohol dehydrogenase in graphene/bovine serum albumin composite film [19], or via glutaraldehyde crosslinking of glucose dehydrogenase for the quantification of glucose and NADH on platinum electrodes [20]. Other strategies include the use of electrodeposited redox hydrogels for the immobilization of GDH and detection of NADH and glucose [4]. The system here proposed is based on the

* Corresponding author at: Department of Chemical Engineering, Faculty of Science and Engineering, Swansea University, Bay Campus, Crymlyn Burrows, Swansea SA1 8EN, United Kingdom.
E-mail address: p.bertoncello@swansea.ac.uk (P. Bertoncello).

https://doi.org/10.1016/j.bioelechem.2023.108365
Received 11 August 2022; Received in revised form 2 January 2023; Accepted 2 January 2023
Available online 5 January 2023

interaction of the immobilized dehydrogenase enzymes with the substrate and the cofactor NAD^+ [21–23]. NAD^+ is constituted by an aromatic amine, which does not generate ECL when reacting with $[Ru(bpy)_3]^{2+}$. Instead, in the case of the NADH structure, the aromaticity of the pyridine group is destroyed during the electrochemical reaction, leading to the formation of an aliphatic tertiary amine which reacts with the $[Ru(bpy)_3]^{2+}$ generating an ECL signal. Herein, we explored the immobilization of the dehydrogenase enzymes into biocompatible alginate hydrogels by studying their selectivity and catalytic action towards the corresponding substrate added to the electrolytic solution containing the cofactor NAD^+ and $[Ru(bpy)_3]^{2+}$. These ECL-based biosensors merge in this way the selectivity of the enzymes along with the sensitivity of the luminophore for the analytical quantification of the corresponding substrate.

2. Experimental

2.1. Reagents

Glucose dehydrogenase (GDH) from *Pseudomonas* sp., lactate dehydrogenase (LDH) from rabbit muscles; β-nicotinamide adenine dinucleotide from yeast (NAD^+); Tris(2,2′-bipyridyl) ruthenium (II) chloride hexahydrate were purchased from Sigma Aldrich and used as received. D-(+) glucose and L-lactic acid were purchased from Fisher Scientific. The artificial sweat stock solution was prepared by mixing 300 mM NaCl, 40 mM of urea, 100 mM of L-lactic acid, 100 mM of D-(+) glucose and 100 mL of distilled water according to a well-established procedure [24]. Finally, the enzymes solutions were prepared by mixing 1 mg/mL of 0.01 M PBS pH 7.4. All the stock solutions were prepared with deionized water purified using a Milli-Q (18 mΩ cm) purification system.

2.2. Apparatus

The cyclic voltammetry and ECL experiments were performed with a CHI potentiostat model 705E connected to a conventional three-electrode configuration electrochemical cell. The working electrodes were glassy carbon electrodes (GCE, 3 mm diameter) purchased from IJ Cambria. The reference electrode was an Ag/AgCl (saturated KCl), with a platinum wire serving as counter electrode. The ECL emission was detected through the PMT purchased from Hamamatsu model H10721-20 biased at 530 V and placed in the direction of the working electrode surface.

2.3. Preparation of the modified GCE

Before deposition of alginate hydrogels, the GCEs were polished using 0.05, 0.3 and 1 μm α-alumina slurry. Afterwards, the GCEs were sonicated to remove all the impurities from the slurry and rinsed with deionized water. Finally, the GCEs were dried with compressed air. The encapsulation of GDH and LDH within alginate hydrogels was performed using the procedure we reported previously related to the encapsulation of oxidases in the alginate hydrogels and that we adapted here for the hydrogenases[25]. Briefly, the enzymes were firstly entrapped into $CaCO_3$ microspheres matrices by co-precipitation of the two salts $CaCl_2$ and Na_2CO_3 forming, according to the Volodkin's process, $CaCO_3$ vaterite microspheres [26]. A layer-by-layer process was performed by alternating two polyelectrolytes, poly (dimethyldiallyammonium chloride) (PDDA) and poly (sodium 4-styrene-sulfonate) (PSS). In doing so, a thin layer with dimensions ranged between 5 and 1000 nm is formed around the $CaCO_3$ microspheres, as result of the electrostatic interaction between the negative and positive charges of the two polyelectrolytes [27–29]. These nanomaterials were then encapsulated within the alginate hydrogels obtained from a 2% alginic salt solution. 3 μL of hydrogels were drop casted on the GCE surface and left to dry at room temperature for 2 h. Afterwards, the crosslinking process was performed by drop casting D-Glucono-1,5-lactone (GDL) to dissociate the $CaCO_3$ molecules and release Ca^{2+} ions [30,31]. The electrode was dried for the second time at room temperature overnight resulting in a successful modification of the electrode [25].

3. Results and discussion

3.1. Optimization of the experimental conditions

The diffusion of the luminophore within the alginate hydrogels without encapsulation of the hydrogenases was studied by recording the CVs at different scan rates and plotting the anodic peak currents vs. the scan rates. The results reported in S1 show a linear dependence of the anodic peak currents vs. the square root of the scan rate indicating that the redox process is diffusion-controlled [33]. The diffusion coefficient of the luminophore at the modified alginate hydrogel GCE was calculated as $D_{hydrogel} = (1.25 \pm 0.4) \times 10^{-7}$ cm^2 s^{-1}, whereas the diffusion coefficient at the bare GCE was $D = (3 \pm 0.2) \times 10^{-6}$ cm^2 s^{-1}. The value of the diffusion coefficient at the bare GCE is consistent with the value ($D = (5.14 \pm 0.1) \times 10^{-6}$ cm^2 s^{-1}) reported by Leddy et al. [32]. As expected, the value of D for the modified alginate GCE is slightly lower than the value of D of the redox probe at the unmodified GCE. This confirms that the luminophore diffuses easily at the GCE surface despite the presence of the alginate on the GCE surface. This fact is not surprising as the alginate hydrogels swell when immersed in aqueous solution allowing ingress and egress of the luminophore with ease [33].

The pH of the electrolytic solutions represented one of the essential parameters for the optimization of the perspective biosensor along with the concentration of NAD^+ and $[Ru(bpy)_3]^{2+}$. It is well known that the pH for maximum GDH activity is 8.0 [34], whereas for LDH, higher activity occurs in the range of pH 7.0–7.8 [35]. Fig. 1 shows the CVs of the alginate hydrogels with encapsulated GDH (A) and LDH (C) recorded in the presence of the corresponding concentration of substrate (glucose and lactic acid, respectively). The peaks (I) observed at 0.7 V correspond to the irreversible oxidation of NADH to NAD^+.

The intensity of this peak increases with the concentration of substrates (glucose and lactic acid). In fact, NADH is the resulting product of the enzymatic reaction of NAD^+ with glucose (Fig. 1A) and lactic acid (Fig. 1C), according to a well-established mechanism summarised in Scheme 1 and 2, whereas the peaks (II) observed at *ca.* +1.1 V correspond to the oxidation of $[Ru(bpy)_3]^{2+}$ to $[Ru(bpy)_3]^{3+}$.

It is well established that dehydrogenase enzymes are cofactor dependent, hence NAD^+ is needed for the catalytic reaction to occur. In doing so, NAD^+ undergoes reduction to NADH with the concomitant oxidation of the glucose to glucono-1,5-lactone (for GDH) and of L-lactic acid to pyruvate (for LDH). Then, the oxidation of NADH to NAD^+ followed by deprotonation generates radical $NAD^{\cdot}$. The reaction of the radical $NAD^{\cdot}$ with the luminophore $[Ru(bpy)_3]^{3+}$ leads to the formation of an excited state, $[Ru(bpy)_3]^{2+*}$ which in turn produces an ECL signal at 610 nm with concomitant regeneration of $[Ru(bpy)_3]^{2+}$.

It is worth to note the resulting broad ECL peak that a more detailed analysis reported in S2 show to be the result of the sum of two distinct ECL peaks observed at +1.1 V (peak I) and +1.4 V (peak II). While peak I corresponds to the emission of light from $[Ru(bpy)_3]^{2+*}$ and NADH as coreactant, instead peak II is likely due to the emission from $[Ru(bpy)_3]^{2+*}$ and some radical species formed at 1.4 V as coreactants which are formed from the electrochemical oxidation of water occurring at such high potential. The identification of such radical species is still subject of intense debate in literature, as the mechanism of water oxidation in alkaline media is still unclear [36,37].

Moreover, according to Park et al. [38], NAD^+ is unstable at very alkaline pH (from pH 9 to 11), hence it is crucial to find a compromise to allow the enzymatic oxidation of the corresponding substrate into products with the concomitant reduction of the cofactor in NADH in a stable environment, while obtaining a good ECL signal. The pH has an important role for the ECL response, particularly the highest ECL

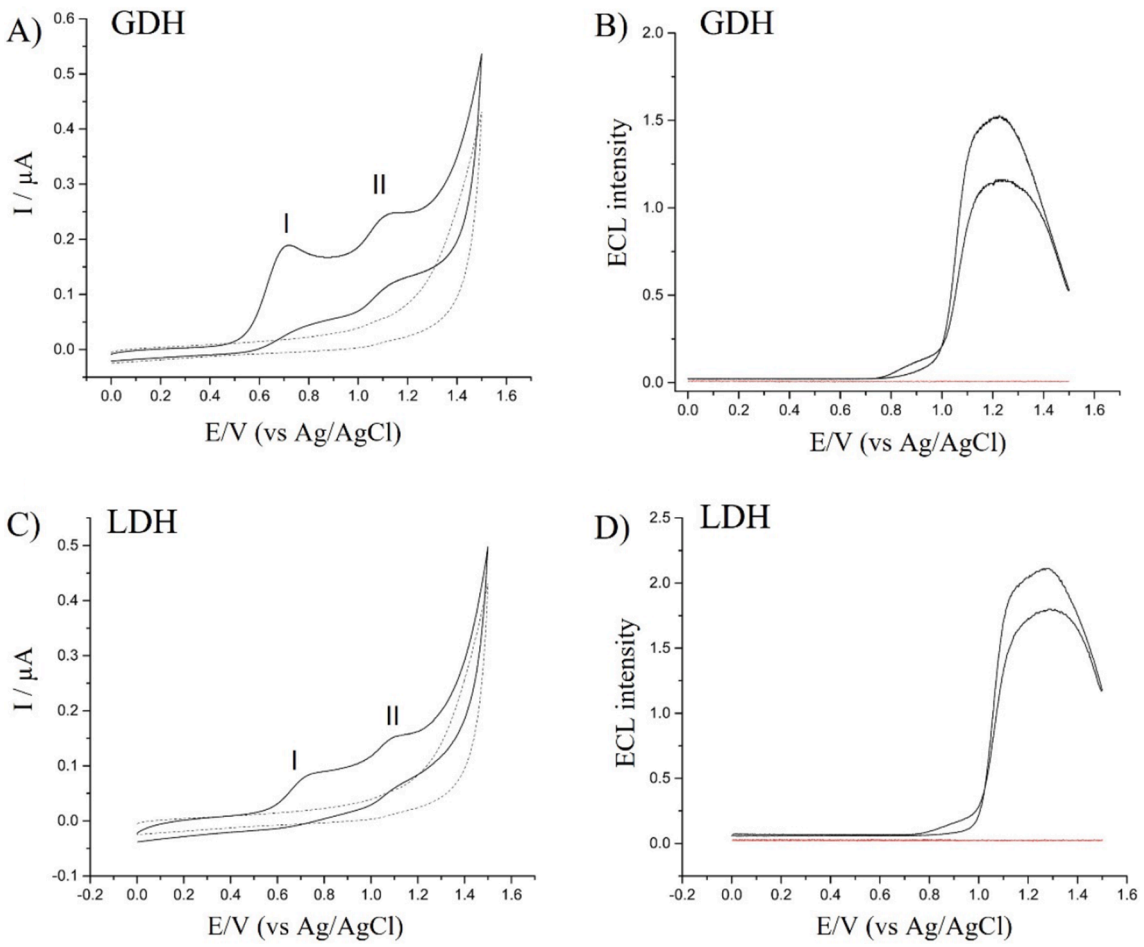

Fig. 1. CVs (A, C) and ECL curves (B, D) for GDH and LDH immobilized in alginate hydrogels. Supporting electrolyte: 0.01 M PBS (pH 7.4) containing 1 mM NAD^+, 2.5 mM $[Ru(bpy)_3]^{2+}$ and 3.36 µM glucose (A, B) and 10 µM of L-lactic acid (C, D); scan rate: 0.05 Vs^{-1}. Dashed and red traces represent the baseline of the CVs and ECL curves respectively. (For interpretation of the references to colour in this figure legend, the reader is referred to the web version of this article.)

$$[Ru(bpy)_3]^{2+} \leftrightarrow [Ru(bpy)_3]^{3+} + e^- \quad (1)$$

$$Glucose + NAD^+ \xrightarrow{GDH} glucono - 1{,}5 - lactone + NADH + H^+ \quad (2)$$

$$NADH \rightarrow NADH^{\cdot+} + e^- \quad (3)$$

$$NADH^{\cdot+} \rightarrow NAD^{\cdot} + H^+ \quad (4)$$

$$[Ru(bpy)_3]^{3+} + NAD^{\cdot} \rightarrow [Ru(bpy)_3]^{2+*} + NAD^+ \quad (5)$$

$$[Ru(bpy)_3]^{2+*} \rightarrow [Ru(bpy)_3]^{2+} + hv \ (610\,nm) \quad (6)$$

Scheme 1. Schematic of the electrochemical and ECL reactions involved with GDH.

$$[Ru(bpy)_3]^{2+} \leftrightarrow [Ru(bpy)_3]^{3+} + e^- \quad (7)$$

$$L - lactic\ acid + NAD^+ \xrightarrow{LDH} pyruvate + NADH + H^+ \quad (8)$$

$$NADH \rightarrow NADH^{\cdot+} + e^- \quad (9)$$

$$NADH^{\cdot+} \rightarrow NAD^{\cdot} + H^+ \quad (10)$$

$$[Ru(bpy)_3]^{3+} + NAD^{\cdot} \rightarrow [Ru(bpy)_3]^{2+*} + NAD^+ \quad (11)$$

$$[Ru(bpy)_3]^{2+*} \rightarrow [Ru(bpy)_3]^{2+} + hv \ (610\,nm) \quad (12)$$

Scheme 2. Schematic of the electrochemical and ECL reactions involved with LDH.

emissions are recorded close to the pK_a value of NAD^+ which is 6.38 [39]. Another factor to consider for the determination of the working pH is the optimum pH at which the enzyme catalyzes the reaction with the corresponding substrate, which is established at pH 8.5 for GDH [34] and pH 7.4 for LDH [40] according to literature. For both enzymes, the ECL experiments were carried out at values of pH in the range 6–9.0 using a scan rate of 0.05 V s^{-1}. Fig. 2 illustrates the ECL response obtained at different values of pH with the highest values for the GDH and LDH obtained in the range of pH 7.5–8.5, and 7.0–7.5, respectively. These results are in agreement with previous works [41–43]. The ECL emission increases in the range from pH 6.0 to 8.0 for GDH and from 6.0 to 7.0 for LDH as the buffer solution has a pH close to the pKa of NAD^+ and close in both cases to the optimum pH of the two enzymes. The ECL signals recorded are therefore, the result of both the enzymes catalysis and the NAD^+ conversion to NADH. Noticeably, at more alkaline values of pH (e.g. pH = 8 for GDH and pH = 7 for LDH), the ECL response decreases as NAD^+ become unstable [44].

For these reasons, we selected pH 8.0 for GDH and pH 7.4 for the LDH in all forthcoming ECL experiments.

Furthermore, the concentrations of the NAD^+ and $[Ru(bpy)_3]^{2+}$ in solution were also investigated. The electrochemical behavior of NAD^+ was studied in the range 0.25–3.0 mM in 0.01 M PBS containing 3.36 µM of glucose for the GDH and 10 µM of L-lactic acid for LDH. Fig. 3 shows that the ECL intensity increased significantly with the cofactor concentration showing a higher conversion to NADH during the enzymatic reaction. The highest response was obtained at a concentration of NAD^+ equal to 2.5 mM. The increase in the ECL response can be attributed to

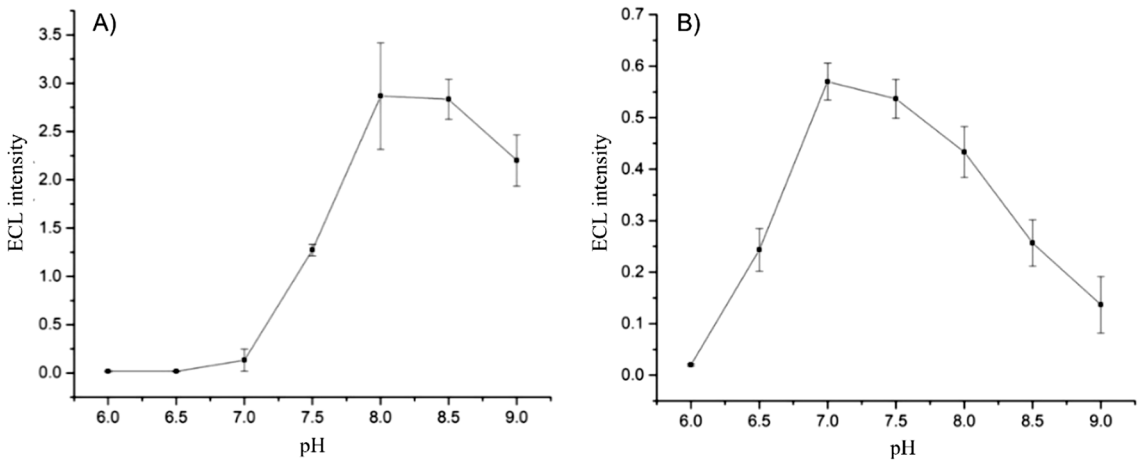

Fig. 2. ECL response vs. pH for GDH (A) and LDH (B) incorporated within alginate hydrogels obtained in 0.01 M PBS supporting electrolyte containing 1 mM NAD^+ and 2.5 mM $[Ru(bpy)_3]^{2+}$. The concentration of glucose and L-lactic acid are 3.36 μM and 10 μM, respectively. Scan rate: 0.05 Vs^{-1}. The errors bar represents triplicate data points.

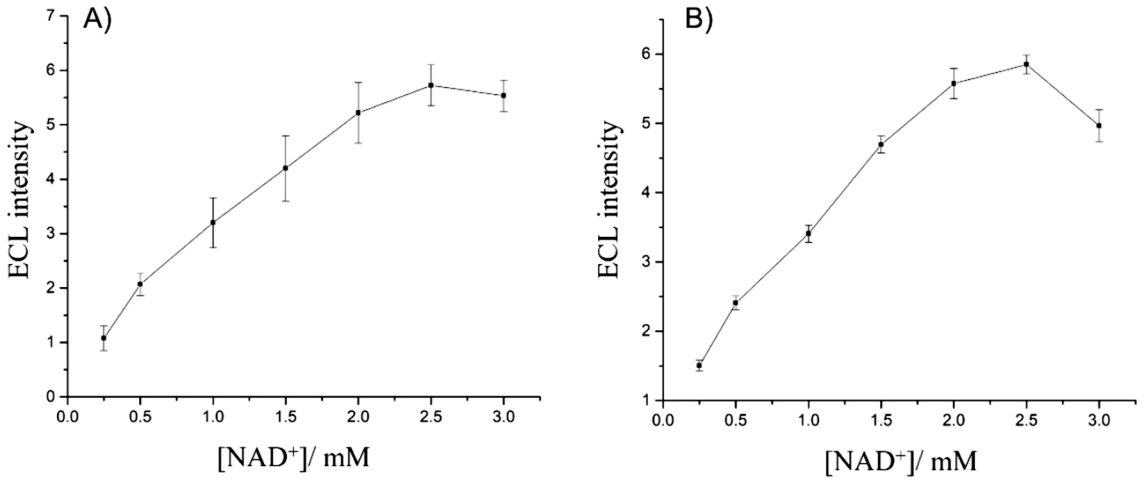

Fig. 3. ECL response vs. cofactor NAD^+ concentration for (A) GDH and (B) LDH immobilized in alginate hydrogels. Supporting electrolyte: 0.01 M PBS; scan rate 0.05 Vs^{-1}. Other conditions: pH 8.0 for GDH (A), and pH 7.4 for LDH (B). Error bars represent triplicate data points.

the higher conversion of NAD^+ to NADH during the reaction catalyzed by the immobilized enzymes [45,20]. To minimize the use of the cofactor due to its cost, a concentration of 1 mM was selected as this value provided good stability and reproducibility of the measurements [46,47].

Finally, the concentration of the luminophore was investigated in the

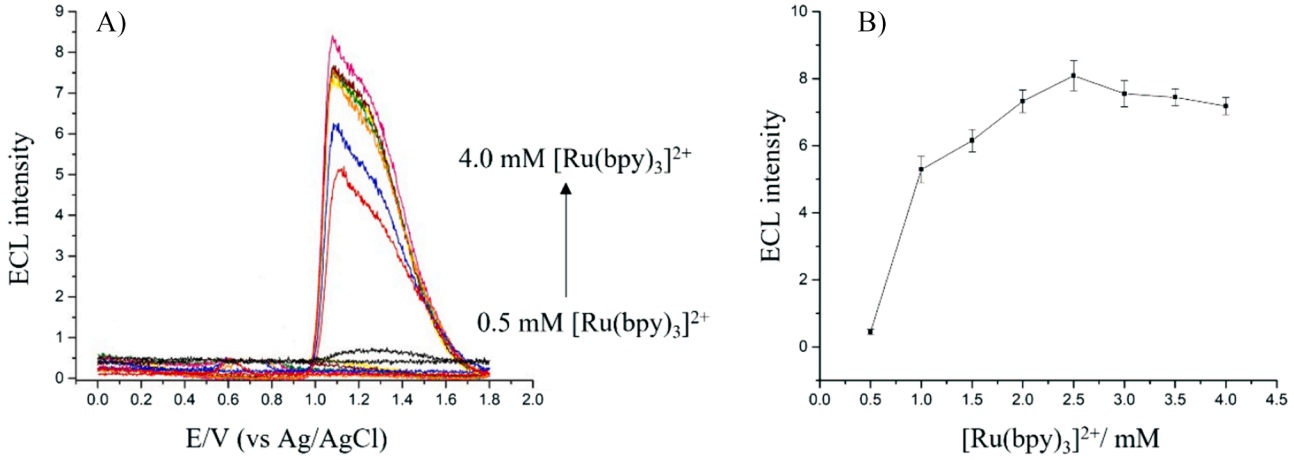

Fig. 4. ECL vs. concentration of $[Ru(bpy)_3]^{2+}$ (A) and corresponding plot (B) recorded in 0.01 M PBS (pH 7.4) containing 1 mM NADH; scan rate 0.05 Vs^{-1}. Error bars represent triplicate data points.

range 0.5–4 mM in 0.01 M PBS at pH 7.4, while maintaining constant the concentration of the cofactor NAD^+ at 1 mM. The results are depicted in Fig. 4. As expected, the ECL intensity increased with the concentration of the luminophore, reaching a plateau at a concentration of 2.5 mM. This is likely due to the diffusion limitations of the luminophore at the electrode surface. As a result, a concentration of luminophore of 2.5 mM was selected for the forthcoming ECL tests.

3.2. Electrochemistry and ECL detection of NADH

To test the suitability of the alginate hydrogels with the incorporated enzymes towards sensing applications, several ECL curves at increasing concentrations of the substrates were recorded. Fig. 5 show the ECL response obtained at different concentrations of glucose (Fig. 5A) and lactic acid (Fig. 5C), respectively. The ECL signal increased linearly with the concentration of the substrates with the curves plateauing as expected at higher concentrations of substrates. The calibrations curves (Fig. 5B and 5D) were obtained from the mean and standard deviation study of three repetitions for each enzyme. The linear range for the GDH-sensor was found in the range 0.52–3.36 μM and the regression equation was y = 0.163 × + 0.22 (R^2 = 0.99), instead for the LDH-system the linear range was between 5 and 20 μM with a regression equation y = 0.162 × - 0.076 (R^2 = 0.99).

These results point out the possibility to detect glucose and lactic acid monitoring the ECL signal of NADH produced from the catalytic reactions of the immobilized enzymes as shown in Scheme 1 and Scheme 2. For GDH, the ECL peak increases linearly with the concentration of glucose up to 4.6 μM reaching a plateau for higher concentrations. Instead, for LDH, the ECL peak increases linearly with the concentration of lactic acid up to 20 μM, then the ECL peak does not change significantly for higher concentrations.

3.3. Interferences study

We assessed the ECL behaviour of the two biosensors in the presence of the most common interfering species typically found in human fluids such as ascorbic acid, glucose, uric acid, dopamine and urea. Fig. 6 summarised the results obtained using a constant concentration of glucose (3.36 μM) and lactic acid (10 μM) in the presence of an excess of interfering species whose concentration was 10 mM. Both GDH and LDH did not show any significant interference with the ECL signal showing high selectivity in the presence of the corresponding substrate.

3.4. Real sample analysis

To test the reliability and specificity of GDH and LDH immobilised within the alginate hydrogels, electrochemical tests were performed using artificial sweat. The influence of glucose and lactic acid concentrations on the ECL signal response were investigated over the range of concentration 0.5–4.5 mM of artificial sweat. This range has been selected based on the average levels of glucose (0.1–1.11 mM) and lactic acid (up to 20 mM) typically found in sweat and reported in literature [48,49].

Fig. 7 reported the CVs (A, D) and ECL curves (B, E) recorded in artificial sweat containing 0.01 M PBS at pH 8.0 supporting electrolyte for GDH-glucose, and pH 7.4 for LDH-lactic acid systems. During the ECL

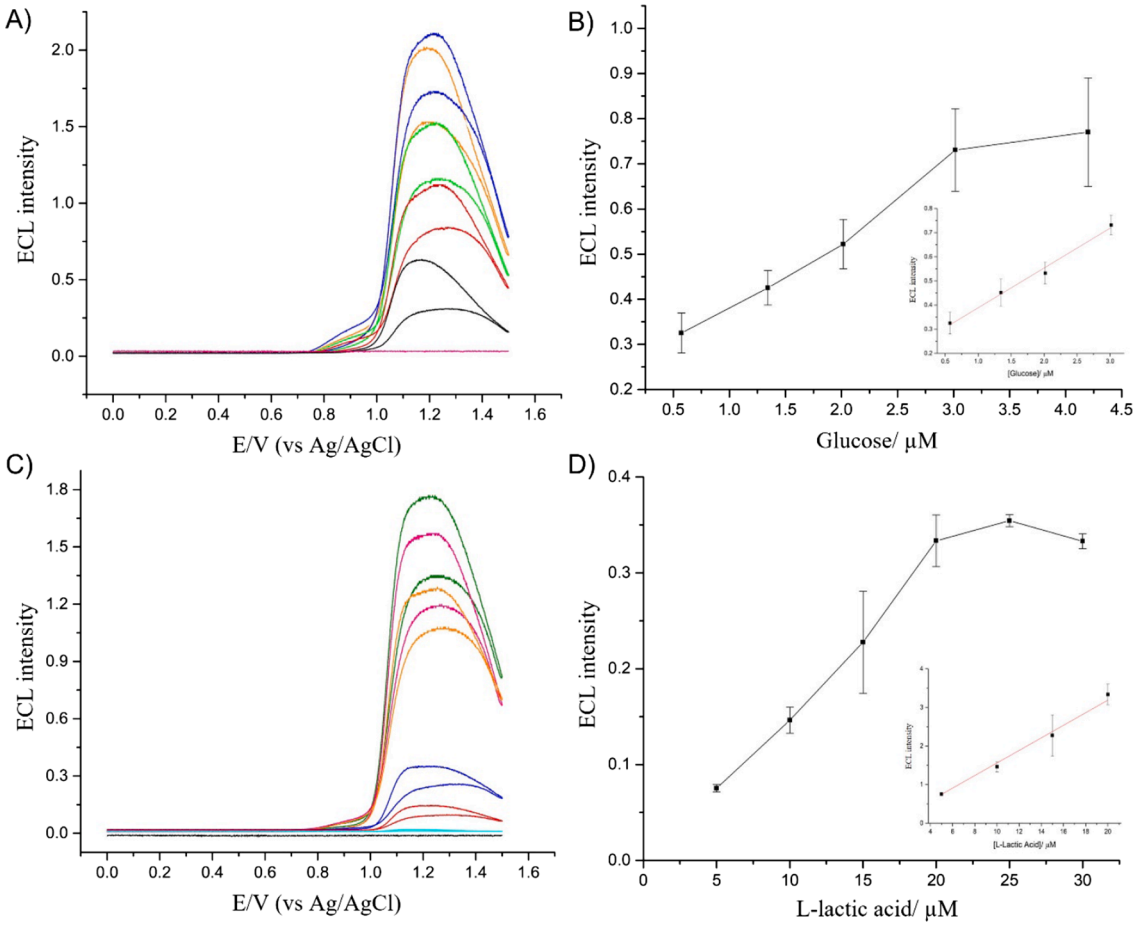

Fig. 5. ECL response of GDH (A) and LDH (C) immobilized into alginate hydrogels. The concentration ranges of glucose and lactic acid are 0.56–4.2 μM and 5–30 μM, respectively. Supporting electrolyte: 0.01 M PBS (pH = 8 for GDH and pH = 7.4 for LDH). The concentration of NAD^+ and $[Ru(bpy)_3]^{2+}$ are 1 mM and 2.5 mM, respectively. The calibration curves (B, D) were obtained from three repetitions of the ECL experiments with the error bars representing triplicate data points.

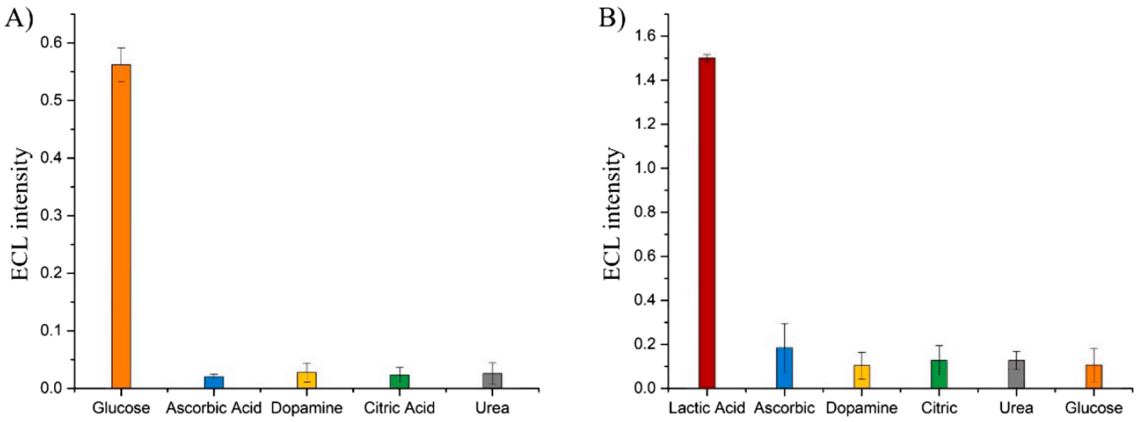

Fig. 6. Interference study for the GDH (A) and LDH (B) recorded in 0.01 M PBS supporting electrolyte (pH 8.0) and (pH 7.4) respectively, containing 1 mM NAD^+ and 2.5 mM $[Ru(bpy)_3]^{2+}$; The concentration of the interference species is 10 mM, whereas the concentration of glucose and lactic acid are 3.36 μM and 10 μM, respectively; Scan rate 0.05 Vs^{-1}. Error bars represent triplicate data points.

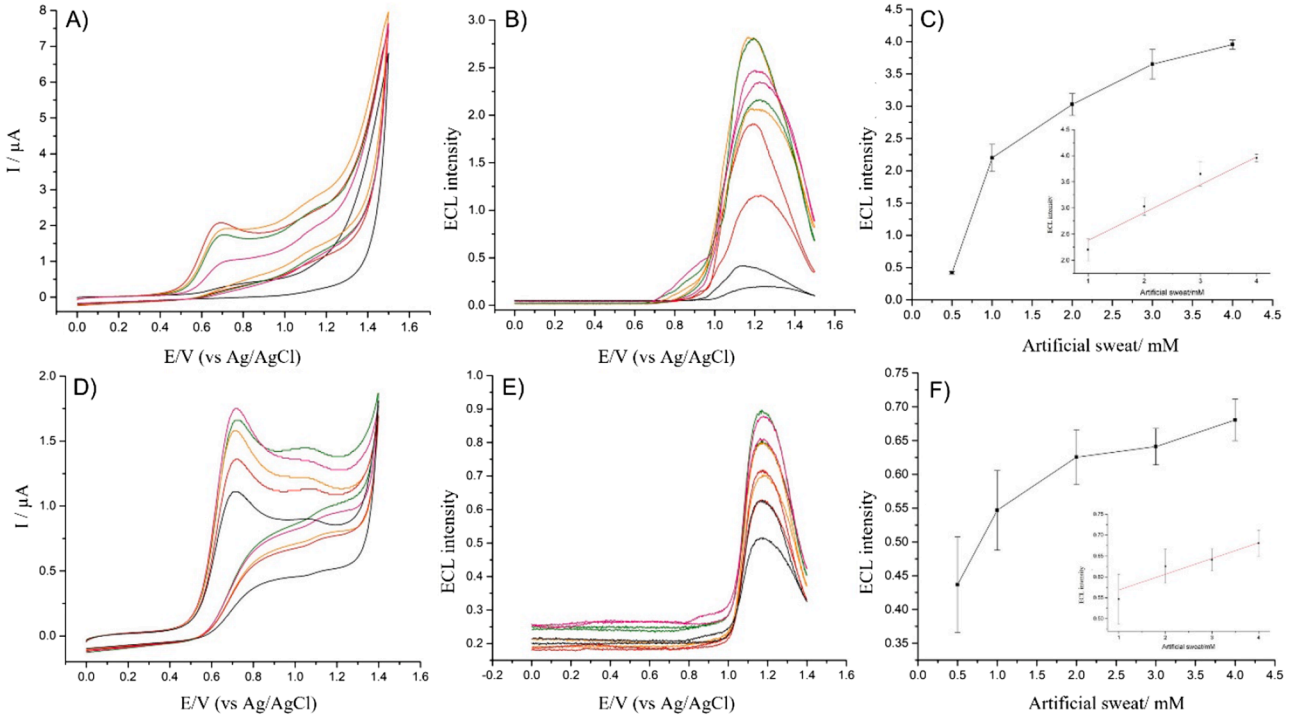

Fig. 7. CVs (A, D) and ECL curves (B, E) vs. artificial sweat concentration for the GDH (A, B) and LDH (D, E) recorded in 0.01 M PBS supporting electrolyte (pH 8.0, GDH, and pH 7.4, LDH) containing 2.5 mM $[Ru(bpy)_3]^{2+}$ and 1 mM NAD^+; scan rate 0.05 Vs^{-1}. Calibration curves for GDH (C) and LDH (F) obtained from the mean and standard deviation of three repetitions of ECL tests performed.

analysis no substrate was added to the electrolytic solution as both glucose and the lactic acid were already included into the stock solution of artificial sweat. The CVs showed the appearance of the peak related to the irreversible oxidation of NADH to NAD^+ at *ca.* 0.7 V and a much less pronounced peak at 1.1 V corresponding to the oxidation of $[Ru(bpy)_3]^{2+}$ to $[Ru(bpy)_3]^{3+}$. As expected, the ECL emission occurred at the potential of oxidation of the luminophore based on the reactions reported in Scheme 1 and 2. The calibration curves reported in Fig. 7(C, F) show that the ECL responses are linear in the presence of different concentrations of artificial sweat. Three repetitions for each system were performed and with the mean and standard deviation calculated in the curves. The limit of detections LOD were calculated following the 3.3 $\delta b/m$ method, where "m" represents the slope of the linear range of the calibration curve and "δb" is the estimated standard deviation of the intercept. The LOD values calculated were 0.93 mM for the GDH-system and 0.59 mM for the LDH. The linear range for GDH was between 1 and 3 mM ($R^2 = 0.98$), instead for the LDH system it was ranged between 1 and 4 mM ($R^2 = 0.98$).

The sensor reproducibility and repeatability were also tested by studying the standard deviation of the ECL emission of the two systems for six replicate measurements on six different GCEs (see Supporting Information, S3). A 4 mM concentration of artificial sweat was added to the electrolytic solution and the repeatability was calculated as 3.03% for the GDH-system and 4.9% for the LDH-system. Finally, in order to establish the accuracy of the proposed biosensors, the modified GCEs were tested for the detection of glucose and L-lactic acid by using the artificial sweat solution spiked with known concentrations of the two substrates (Table 1).

The data reported in Table 1 showed that the recovery for the GDH- and LDH-systems was 98% and 99%, respectively. These results

Table 1
Calculated glucose and L-lactic acid concentrations and % recoveries obtained from ECL analysis of spiked artificial sweat diluted in 0.01 M PBS at pH 8 (GDH) and pH 7.4 (LDH).

Sample	Avg concn calcd	Recovery %
Glucose spiked artificial sweat solution	2.38 μM	98%
L-lactic acid spiked artificial sweat solution	9.01 μM	99%

demonstrate a high degree of accuracy of the ECL sensor with recoveries above the 95% threshold required for analytical methods [44].

4. Conclusions

In summary, we have demonstrated the incorporation of dehydrogenases such as GDH and LDH within alginate hydrogels. These enzymes incorporated within alginate hydrogels were deposited on glassy carbon electrodes and used for the ECL detection of glucose and lactic acid throughout the conversion of NAD^+ to NADH and concomitant oxidation of glucose and lactic acid operated by GDH and LDH. The GDH- and LDH-biosensors showed suitable response for glucose and lactic acid concentrations. The biosensors, validated utilizing artificial sweat solution to simulate real scenario, showed good reproducibility for both GDH- and LDH- systems. The results herein presented could be improved by mean of immobilisation of the luminophore into a thin polymeric matrix which will be the subject of future investigations.

In this respect, further studies are required for the immobilization of the luminophore and NAD^+ within polymeric matrices to develop a complete solid-state ECL biosensor and, in doing so, minimizing the use of such expensive reagents. These as-prepared biosensors represent a promising route for the development of non-invasive, low-cost, and real-time disposable ECL-based biosensors.

Declaration of Competing Interest

The authors declare that they have no known competing financial interests or personal relationships that could have appeared to influence the work reported in this paper.

Data availability

Data will be made available on request.

Acknowledgments

L.S.F. gratefully acknowledges financial support from a Knowledge Economy Skills PhD Scholarship (KESS2) under the Welsh Government's European Social Fund (ESF) convergence programme for West Wales and the Valleys and Perpetuus Carbon Ltd. P.B. acknowledges the Institute for Innovative Materials, Processing and Numerical Technologies (IMPACT) for the purchase of the ECL set up.

Appendix A. Supplementary data

Supplementary data to this article can be found online at https://doi.org/10.1016/j.bioelechem.2023.108365.

References

[1] P. Bertoncello, Nanomaterials for biosensing with electrochemiluminescence (ECL) detection, Front. Biosci.-Landmark 16 (2011) 1084–1108.
[2] X.-M. Chen, B.-Y. Su, X.-H. Song, Q.-A. Chen, X. Chen, X.-R. Wang, Recent advances in electrochemiluminescent enzyme biosensors, TrAC Trends Anal. Chem. 30 (2011) 665–676.
[3] H. Qi, C. Zhang, Electrogenerated chemiluminescence biosensing, Anal. Chem. 92 (2019) 524–534.
[4] M. Milutinovic, S. Sallard, D. Manojlovic, N. Mano, N. Sojic, Glucose sensing by electrogenerated chemiluminescence of glucose-dehydrogenase produced NADH on electrodeposited redox hydrogel, Bioelectrochemistry 82 (2011) 63–68.
[5] J.B. Claver, M.V. Mirón, L. Capitán-Vallvey, Disposable electrochemiluminescent biosensor for lactate determination in saliva, Analyst 134 (2009) 1423–1432.
[6] K. Petropoulos, S. Piermarini, S. Bernardini, G. Palleschi, D. Moscone, Development of a disposable biosensor for lactate monitoring in saliva, Sens. Actuators B 237 (2016) 8–15.
[7] M. Zhang, R. Yuan, Y. Chai, S. Chen, H. Zhong, C. Wang, Y. Cheng, A biosensor for cholesterol based on gold nanoparticles-catalyzed luminol electrogenerated chemiluminescence, Biosens. Bioelectron. 32 (2012) 288–292.
[8] L. Dennany, Electrochemiluminescence fundamentals and analytical applications, Electrochemistry: Volume 15, The Royal Society of Chemistry, 2019, pp. 96-146.
[9] L. Dennany, Z. Mohsan, A.L. Kanibolotsky, P.J. Skabara, Novel electrochemiluminescent materials for sensor applications, Faraday Discuss. 174 (2014) 357–367.
[10] R.J. Forster, P. Bertoncello, T.E. Keyes, Electrogenerated chemiluminescence, Annu. Rev. Anal. Chem. 2 (2009) 359–385.
[11] J.K. Leland, Electrogenerated Chemiluminescence: An Oxidative-Reduction Type ECL Reaction Sequence Using Tripropyl Amine, J. Electrochem. Soc., 137 (1990) 3127-3127.
[12] J.B. Noffsinger, N.D. Danielson, Generation of chemiluminescence upon reaction of aliphatic amines with tris (2, 2'-bipyridine) ruthenium (III), Anal. Chem. 59 (1987) 865–868.
[13] S.N. Brune, D.R. Bobbitt, Role of electron-donating/withdrawing character, pH, and stoichiometry on the chemiluminescent reaction of tris (2, 2'-bipyridyl) ruthenium (III) with amino acids, Anal. Chem. 64 (1992) 166–170.
[14] T.M. Downey, T.A. Nieman, Chemiluminescence detection using regenerable tris (2, 2'-bipyridyl) ruthenium (II) immobilized in Nafion, Anal. Chem. 64 (1992) 261–268.
[15] I. Rubinstein, C.R. Martin, A.J. Bard, Electrogenerated chemiluminescent determination of oxalate, Anal. Chem. 55 (1983) 1580–1582.
[16] Z. Xu, Z. Guo, S. Dong, Electrogenerated chemiluminescence biosensor with alcohol dehydrogenase and tris (2, 2′-bipyridyl) ruthenium (II) immobilized in sol–gel hybrid material, Biosens. Bioelectron. 21 (2005) 455–461.
[17] L. Zhang, Z. Xu, X. Sun, S. Dong, A novel alcohol dehydrogenase biosensor based on solid-state electrogenerated chemiluminescence by assembling dehydrogenase to Ru (bpy) 32+–Au nanoparticles aggregates, Biosens. Bioelectron. 22 (2007) 1097–1100.
[18] A.A. Homaei, R. Sariri, F. Vianello, R. Stevanato, Enzyme immobilization: An update, J. Chem. Biol. 6 (2013) 185–205.
[19] W. Gao, Y. Chen, J. Xi, S. Lin, Y. Chen, Y. Lin, Z. Chen, A novel electrochemiluminescence ethanol biosensor based on tris(2,2′-bipyridine) ruthenium (II) and alcohol dehydrogenase immobilized in graphene/bovine serum albumin composite film, Biosens. Bioelectron. 41 (2013) 776–782.
[20] A.F. Martin, T.A. Nieman, Glucose quantitation using an immobilized glucose dehydrogenase enzyme reactor and a tris(2,2′-bipyridyl) ruthenium(II) chemiluminescent sensor, Anal. Chim. Acta 281 (1993) 475–481.
[21] P. Bertoncello, A.J. Stewart, L. Dennany, Analytical applications of nanomaterials in electrogenerated chemiluminescence, Anal. Bioanal. Chem. 406 (2014) 5573–5587.
[22] A. Devadoss, L. Dennany, C. Dickinson, T.E. Keyes, R.J. Forster, Highly sensitive detection of NADH using electrochemiluminescent nanocomposites, Electrochem. Commun. 19 (2012) 43–45.
[23] E.J. O'Reilly, T.E. Keyes, R.J. Forster, L. Dennany, Insights into electrochemiluminescent enhancement through electrode surface modification, Analyst 138 (2013) 677–682.
[24] U.B. Gunatilake, S. Garcia-Rey, E. Ojeda, L. Basabe-Desmonts, F. Benito-Lopez, TiO2 Nanotubes Alginate Hydrogel Scaffold for Rapid Sensing of Sweat Biomarkers: Lactate and Glucose, ACS Appl. Mater. Interfaces 13 (2021) 37734–37745.
[25] L.S. Ferraraccio, D. Di Lisa, L. Pastorino, P. Bertoncello, Enzymes Encapsulated within Alginate Hydrogels: Bioelectrocatalysis and Electrochemiluminescence Applications, Anal. Chem. 94 (2022) 16122–16131.
[26] D. Volodkin, CaCO3 templated micro-beads and -capsules for bioapplications, Adv. Colloid Interface Sci. 207 (2014) 306–324.
[27] A. Blandino, M. Macías, D. Cantero, Glucose oxidase release from calcium alginate gel capsules, Enzyme Microb. Technol. 27 (2000) 319–324.
[28] S. Boi, E. Dellacasa, N. Rouatbi, O. Monticelli, L. Pastorino, Multicompartment Hydrogels for the Local Delivery of Chemotherapic Drugs, pHealth, 2019, pp. 261-265.
[29] M.C. Lamas, C. Bregni, M. Daquino, J. Degrossi, R. Firenstein, Calcium alginate microspheres of Bacillus subtilis, Drug Dev Ind Pharm 27 (2001) 825–829.
[30] F. Abasalizadeh, S.V. Moghaddam, E. Alizadeh, E. Kashani, S.M.B. Fazljou, M. Torbati, A. Akbarzadeh, Alginate-based hydrogels as drug delivery vehicles in cancer treatment and their applications in wound dressing and 3D bioprinting, J. Biol. Eng. 14 (2020) 1–22.
[31] S. Boi, N. Rouatbi, E. Dellacasa, D. Di Lisa, P. Bianchini, O. Monticelli, L. Pastorino, Alginate microbeads with internal microvoids for the sustained release of drugs, Int. J. Biol. Macromol. 156 (2020) 454–461.
[32] K.L. Knoche, C. Hettige, P.D. Moberg, S. Amarasinghe, J. Leddy, Cyclic voltammetric diagnostics for inert, uniform density films, J. Electrochem. Soc. 160 (2013) H285.
[33] A.J. Bard, L.R. Faulkner, Electrochemical methods: fundamentals and applications, John Wiley & Sons, New York, 2022, p. 226.

[34] Y. Fujita, R. Ramaley, E. Freese, Location and properties of glucose dehydrogenase in sporulating cells and spores of Bacillus subtilis, J. Bacteriol. 132 (1977) 282–293.
[35] J.A. Birkbeck, A. Stewart, The estimation of lactate dehydrogenase activity of human erythrocytes, Can. J. Biochem. Physiol. 39 (1961) 257–265.
[36] C. Hu, L. Zhang, J. Gong, Recent progress made in the mechanism comprehension and design of electrocatalysts for alkaline water splitting, Energ. Environ. Sci. 12 (2019) 2620–2645.
[37] M. Plevová, J. Hnát, K. Bouzek, Electrocatalysts for the oxygen evolution reaction in alkaline and neutral media. A comparative review, J. Power Sources 507 (2021), 230072.
[38] J.-K. Park, H.-J. Yee, K.S. Lee, W.-Y. Lee, M.-C. Shin, T.-H. Kim, S.-R. Kim, Determination of breath alcohol using a differential-type amperometric biosensor based on alcohol dehydrogenase, Anal. Chim. Acta 390 (1999) 83–91.
[39] J. Kvassman, G. Pettersson, Effect of pH on coenzyme binding to liver alcohol dehydrogenase, Eur. J. Biochem. 100 (1979) 115–123.
[40] J. Torres-da Matta, A. Nery da Matta, A. Hassón-Voloch, L(+) lactate dehydrogenase activity from the electric organ of Electrophorus electricus (L.), An Acad. Bras Cienc 48 (1976) 145–151.
[41] P. Du, P. Wu, C. Cai, A glucose biosensor based on electrocatalytic oxidation of NADPH at single-walled carbon nanotubes functionalized with poly(nile blue A), J. Electroanal. Chem. 624 (2008) 21–26.
[42] G. Guo, Q. Chen, X. Chen, Electrochemiluminescence glucose biosensor based on glucose dehydrogenase functionalized Ru(bpy)32+ doped silica nanoparticles, Sci. China Chem. 54 (2011) 1777–1781.
[43] C.-I. Li, Y.-H. Lin, C.-L. Shih, J.-P. Tsaur, L.-K. Chau, Sol–gel encapsulation of lactate dehydrogenase for optical sensing of l-lactate, Biosens. Bioelectron. 17 (2002) 323–330.
[44] K. Brown, M. McMenemy, M. Palmer, M.J. Baker, D.W. Robinson, P. Allan, L. Dennany, Utilization of an Electrochemiluminescence Sensor for Atropine Determination in Complex Matrices, Anal. Chem. 91 (2019) 12369–12376.
[45] R. Appelqvist, G. Marko-Varga, L. Gorton, A. Torstensson, G. Johansson, Enzymatic determination of glucose in a flow system by catalytic oxidation of the nicotinamide coenzyme at a modified electrode, Anal. Chim. Acta 169 (1985) 237–247.
[46] A.F. Martin, Chemiluminescence detection of NADH and enzyme substrates with immobilized tris(2,2'-bipyridyl)ruthenium (II) and dehydrogenase enzymes, Ann Arbor (1995).
[47] Y. Yuan, S. Han, L. Hu, S. Parveen, G. Xu, Coreactants of tris(2,2′-bipyridyl) ruthenium(II) Electrogenerated Chemiluminescence, Electrochim. Acta 82 (2012) 484–492.
[48] S.M. Khor, J. Choi, P. Won, S.H. Ko, Challenges and Strategies in Developing an Enzymatic Wearable Sweat Glucose Biosensor as a Practical Point-Of-Care Monitoring Tool for Type II Diabetes, Nanomaterials 12 (2022) 221.
[49] D. Sakharov, M. Shkurnikov, M.Y. Vagin, E. Yashina, A. Karyakin, A. Tonevitsky, Relationship between lactate concentrations in active muscle sweat and whole blood, Bull. Exp. Biol. Med. 150 (2010) 83.